Ab initio calculations of exchange interactions, spin-wave stiffness constants, and Curie temperatures of Fe, Co, and Ni

M. Pajda,[1] J. Kudrnovský,[2,1] I. Turek,[3,4] V. Drchal,[2] and P. Bruno[1]
[1]*Max-Planck-Institut für Mikrostrukturphysik, Weinberg 2, D-06120 Halle, Germany*
[2]*Institute of Physics, Academy of Sciences of the Czech Republic, Na Slovance 2, CZ-182 21 Prague 8, Czech Republic*
[3]*Institute of Physics of Materials, Academy of Sciences of the Czech Republic, Žižkova 22, CZ-616 62 Brno, Czech Republic*
[4]*Department of Electronic Structures, Charles University, Ke Karlovu 5, CZ-121 16 Prague 2, Czech Republic*
(Received 27 July 2000; revised manuscript received 20 December 2000; published 1 October 2001)

We have calculated Heisenberg exchange parameters for bcc Fe, fcc Co, and fcc Ni using the nonrelativistic spin-polarized Green-function technique within the tight-binding linear muffin-tin orbital method and by employing the magnetic force theorem to calculate total energy changes associated with a local rotation of magnetization directions. We have also determined spin-wave stiffness constants and found the dispersion curves for metals in question employing the Fourier transform of calculated Heisenberg exchange parameters. Detailed analysis of convergence properties of the underlying lattice sums was carried out and a regularization procedure for calculation of the spin-wave stiffness constant was suggested. Curie temperatures were calculated both in the mean-field approximation and within the Green-function random-phase approximation. The latter results were found to be in a better agreement with available experimental data.

DOI: 10.1103/PhysRevB.64.174402 PACS number(s): 75.10.−b, 71.15.−m, 75.30.Ds

I. INTRODUCTION

The quantitative description of thermodynamic properties of magnetic metals is challenging solid-state theorists since decades. Thanks to the development of density-functional theory and its implementation to *ab initio* computational schemes, an excellent understanding of their ground state (i.e., at $T=0$ K) has been achieved. On the other hand, most of the progress towards a description of magnetic metals at nonzero temperature has been based upon models in which the electronic structure is oversimplified and described in terms of empirical parameters. Although this approach has the great merit of emphasizing the relevant mechanisms and concepts, it cannot properly take into account the complex details of the electronic structure and is therefore unable to yield quantitative predictions of the relevant physical quantities such as spin-wave stiffness, Curie temperature T_C, etc., for comparison with experimental data.

It is therefore of a great importance to develop an *ab initio*, parameter-free, scheme for the description of ferromagnetic metals at $T>0$ K. Such an approach must be able to go beyond the ground state and to take into account excited states, in particular the magnetic excitations responsible for the decrease of the magnetization with temperature and for the phase transition at $T=T_C$. Although density-functional theory can be formally extended to nonzero temperature, there exists at present no practical scheme allowing to implement it. One therefore has to rely on approximate approaches. The approximations to be performed must be chosen on the basis of physical arguments.

In itinerant ferromagnets, it is well known that magnetic excitations are basically of two different types.

(i) Stoner excitations, in which an electron is excited from an occupied state of the majority-spin band to an empty state of the minority-spin band and creates an electron-hole pair of triplet spin. They are associated with longitudinal fluctuations of the magnetization.

(ii) The spin waves or magnons, which correspond to collective transverse fluctuations of the direction of the magnetization. Near the bottom of the excitation spectrum, the density of states of magnons is considerably larger than that of corresponding Stoner excitations, so that the thermodynamics in the low-temperature regime is completely dominated by magnons and Stoner excitations can be neglected. Therefore it seems reasonable to extend this approximation up to the Curie temperature, and to estimate the latter by neglecting Stoner excitations. This is a good approximation for ferromagnets with a large exchange splitting such as Fe and Co, but it is less justified for Ni that has a small exchange splitting.

The purpose of the present paper is to describe the spin-wave properties of transition metal itinerant ferromagnets at *ab initio* level. With thermodynamic properties in mind, we are primarily interested in the long-wavelength magnons with the lowest energy. We shall adopt the *adiabatic approximation* in which the *precession* of the magnetization due to a spin wave is neglected when calculating the associated change of electronic energy. Clearly, the condition of validity of this approximation is that the precession time of the magnetization should be large as compared to characteristic times of electronic motion, namely, the hopping time of an electron from a given site to a neighboring one, and the precession time of the spin of an electron subject to the exchange field. In other words, the spin-wave energies should be small as compared to the bandwidth and to the exchange splitting. This approximation becomes exact in the limit of long-wavelength magnons, so that the spin-wave stiffness constants calculated in this way are in principle exact.

This procedure corresponds to a mapping of the itinerant electron system onto an effective Heisenberg Hamiltonian with classical spins

$$H_{\mathrm{eff}}=-\sum_{i\neq j} J_{ij}\mathbf{e}_i\cdot\mathbf{e}_j, \tag{1}$$

where J_{ij} is the exchange interaction energy between two particular sites (i,j), and $\mathbf{e}_i, \mathbf{e}_j$ are unit vectors pointing in the direction of local magnetic moments at sites (i,j), respectively. The same point of view has been adopted in various papers recently published on the same topic.[1–14]

The procedure for performing the above mapping onto an effective Heisenberg Hamiltonian relies on the constrained density-functional theory,[15] which allows to obtain the ground-state energy for a system subject to certain constraints. In the case of magnetic interactions, the constraint consists in imposing a given configuration of spin-polarization directions, namely, along $\mathbf{e}_i$ within the atomic cell *i*. Note that *intracell* noncollinearity of the spin polarization is neglected since we are primarily interested in low-energy excitations due to *intercell* noncollinearity.

Once the exchange parameters J_{ij} are obtained, the spin dynamics[4,16,17] can be determined from the effective Hamiltonian (1) and one obtains the result known from spin-wave theories of localized ferromagnets: the spin-wave energy $E(\mathbf{q})$ is related to the exchange parameters J_{ij} by a simple Fourier transformation

$$E(\mathbf{q}) = \frac{4\mu_B}{M} \sum_{j \neq 0} J_{0j}(1 - \exp[i\mathbf{q}\cdot\mathbf{R}_{0j}]), \tag{2}$$

where $\mathbf{R}_{0j} = \mathbf{R}_0 - \mathbf{R}_j$ denote lattice vectors in the real space, $\mathbf{q}$ is a vector in the corresponding Brillouin zone, and M is the magnetic moment per atom (μ_B is the Bohr magneton).

There are basically two approaches to calculate the exchange parameters and spin-wave energies. The first one that we adopt in the present paper, referred to as the real-space approach, consists in calculating directly J_{ij} by employing the change of energy associated with a constrained rotation of the spin-polarization axes in cells *i* and *j*.[2] In the framework of the so-called magnetic force theorem[2,18] the change of the total energy of the system can be approximated by the corresponding change of one-particle energies that significantly simplifies calculations. The spin-wave energies are then obtained from Eq. (2). In the second approach, referred to as the frozen-magnon approach, one chooses the constrained spin-polarization configuration to be the one of a spin wave with the wave vector $\mathbf{q}$ and computes $E(\mathbf{q})$ directly by employing the generalized Bloch theorem for a spin-spiral configuration.[19] Like the above one, approach can be implemented with or without using the the magnetic force theorem. Both the real-space approach and the frozen-magnon approach can be implemented by using either a finite or an infinitesimal rotation, the latter choice is usually preferable. The exchange parameters J_{ij} are then obtained by inverting Eq. (2). One should also mention a first-principles theory of spin fluctuations (the so-called disordered local-moment picture) based on the idea of a generalized Onsager cavity field.[20]

The spin-wave stiffness *D* is given by the curvature of the spin-wave dispersion $E(\mathbf{q})$ at $\mathbf{q}=0$. Although its calculation is in principle straightforward in the real-space approach, we shall show that serious difficulties arise due to the Ruderman-Kittel-Kasuya-Yoshida (RKKY) character of magnetic interactions in metallic systems. These difficulties have been underestimated in a number of previous studies,[2,5,13,14] and the claimed agreement with experiment is thus fortituous. We shall present a procedure allowing to overcome these difficulties. In addition, we shall demonstrate that the evaluation of the spin-wave dispersion $E(\mathbf{q})$ in the real-space approach has to be also done carefully with respect to the convergency of results with the number of shells included.

Finally, to obtain thermodynamic quantities such as the Curie temperature, we apply statistical mechanics to the effective Hamiltonian (1). In the present paper, we use two different approaches to compute the Curie temperature. The first one is the commonly used mean-field approximation (MFA). The limitations of this method are well known: it is correct only in the limit of high temperatures (above T_C), and it fails to describe the low-temperature collective excitations (spin waves). The second approach is the Green-function method within the random-phase approximation (RPA).[21–26] The RPA is valid not only for high temperatures, but also at low temperatures, and it describes correctly the collective excitations (spin waves). In the intermediate regime (around T_C), it represents a rather good approximation that may be viewed as an interpolation between the high- and low-temperature regimes. It usually yields a better estimate of the Curie temperature as compared to the MFA. It should be noted, however, that both the MFA and RPA fail to describe correctly the critical behavior and yield in particular incorrect critical exponents.

II. FORMALISM

The site-off diagonal exchange interactions J_{ij} are calculated using the expression[2]

$$J_{ij} = \frac{1}{4\pi} \mathrm{Im} \int_C \mathrm{tr}_L[\{P_i^{\uparrow}(z) - P_i^{\downarrow}(z)\} g_{ij}^{\uparrow}(z) \times \{P_j^{\uparrow}(z) - P_j^{\downarrow}(z)\} g_{ji}^{\downarrow}(z)] dz, \tag{3}$$

which is evaluated in the framework of the first-principles tight-binding linear muffin-tin orbital method (TB-LMTO).[27] Here tr_L denotes the trace over the angular momentum $L=(lm)$, energy integration is performed in the upper half of the complex energy plane over a contour *C* starting below the bottom of the valence band and ending at the Fermi energy, $P_i^{\sigma}(z)$ are diagonal matrices of the so-called potential functions of the TB-LMTO method for a given spin direction $\sigma = \uparrow, \downarrow$ with elements $P_{i,L}^{\sigma}(z)$, and $g_{ij}^{\sigma}(z)$ are the so-called auxiliary Green-function matrices with elements $g_{iL,jL'}^{\sigma}(z)$ (Ref. 28) defined as

$$[g^{\sigma}(z)]_{iL,jL'}^{-1} = P_{i,L}^{\sigma}(z)\,\delta_{LL'}\,\delta_{i,j} - S_{iL,jL'}. \tag{4}$$

We have also introduced the spin-independent screened structure constant matrix $S_{i,j}$ with elements $S_{iL,jL'}$ that characterizes the underlying lattice within the TB-LMTO approach.[28]

Calculated exchange parameters were further employed to estimate the spin-wave spectrum $E(\mathbf{q})$ as given by Eq. (2). For cubic systems and in the range of small $\mathbf{q}$ we have

$$E(\mathbf{q}) = Dq^2, \tag{5}$$

where $q = |\mathbf{q}|$. The spin-wave stiffness coefficient D can be expressed directly in terms of the exchange parameters J_{0j} as[2]

$$D = \frac{2\mu_B}{3M} \sum_j J_{0j} R_{0j}^2, \tag{6}$$

where $R_{0j} = |\mathbf{R}_{0j}|$. The summation in Eq. (6) runs over all sites but in practice the above sum has to be terminated at some maximal value of $R_{0j} = R_{max}$. There is a lot of misunderstanding in the literature as concerns the use of Eq. (6). Several calculations were done with R_{max} corresponding to the first few coordination shells.[2,13,14] In other calculations[14,5] the authors realized the problem of the termination of R_{max} but they did not suggest an appropriate method to perform the sum (6) in the direct space. We will demonstrate that terminating the sum in Eq. (6) after some value of R_{max} is fundamentally incorrect because it represents a nonconverging quantity and we will show how to resolve this problem from a numerical point of view. The reason for such behavior is the long-range oscillatory character of J_{ij} with the distance R_{ij} in ferromagnetic metals.

Alternatively, it is possible to evaluate $E(\mathbf{q})$ directly in the reciprocal space[5] as

$$E(\mathbf{q}) = \frac{4\mu_B}{M}[J(\mathbf{0}) - J(\mathbf{q})],$$

$$J(\mathbf{q}) = \frac{1}{4\pi N} \mathrm{Im} \sum_{\mathbf{k}} \int_C \mathrm{tr}_L[\{P^{\uparrow}(z) - P^{\downarrow}(z)\} g^{\uparrow}(\mathbf{k}+\mathbf{q}, z) \times \{P^{\uparrow}(z) - P^{\downarrow}(z)\} g^{\downarrow}(\mathbf{k}, z)] dz, \tag{7}$$

and to determine the spin-stiffness constant as a second derivative of $E(\mathbf{q})$ with respect to $\mathbf{q}$.

Calculated exchange parameters can be also used to determine Curie temperatures of considered metals. Within the MFA

$$k_B T_C^{MFA} = \frac{2}{3} \sum_{j \neq 0} J_{0j} = \frac{M}{6\mu_B} \frac{1}{N} \sum_{\mathbf{q}} E(\mathbf{q}), \tag{8}$$

where $E(\mathbf{q})$ is the spin-wave energy (2). We have calculated T_C^{MFA} directly from the expression $k_B T_C^{MFA} = 2J_0/3$, where[2]

$$J_0 \equiv \sum_{i \neq 0} J_{0i} = -\frac{1}{4\pi} \int_C \mathrm{Im}\ \mathrm{tr}_L[\{P_0^{\uparrow}(z) - P_0^{\downarrow}(z)\} \times \{g_{00}^{\uparrow}(z) - g_{00}^{\downarrow}(z)\} + \{P_0^{\uparrow}(z) - P_0^{\downarrow}(z)\} g_{00}^{\uparrow}(z) \times \{P_0^{\uparrow}(z) - P_0^{\downarrow}(z)\} g_{00}^{\downarrow}(z)] dz. \tag{9}$$

The expression for the Curie temperature within the (Green-function) GF-RPA approach is[26]

$$\frac{1}{k_B T_C^{RPA}} = \frac{6\mu_B}{M} \frac{1}{N} \sum_{\mathbf{q}} \frac{1}{E(\mathbf{q})}. \tag{10}$$

The integrand in Eq. (10) is singular for $\mathbf{q} = 0$. We have therefore calculated T_C^{RPA} using the expression

$$\frac{1}{k_B T_C^{RPA}} = -\lim_{z \to 0} \frac{6\mu_B}{M} \mathrm{Re}\, G_m(z),$$

$$G_m(z) = \frac{1}{N} \sum_{\mathbf{q}} \frac{1}{z - E(\mathbf{q})}. \tag{11}$$

The quantity $G_m(z)$ is the magnon Green function corresponding to the dispersion law $E(\mathbf{q})$ and it was evaluated for energies z in the complex energy plane and its value for $z = 0$ was obtained using the analytical deconvolution technique.[29] It should be noted that the MFA and the RPA differ essentially in the way in which they weight various J_{ij}, namely, more distant neighbors play a more important role in the RPA as compared to the MFA. It is seen from Eqs. (8) and (10) that T_C^{MFA} and T_C^{RPA} are given as the arithmetic and harmonic averages of the spin-wave energies $E(\mathbf{q})$, respectively, and therefore it holds $T_C^{MFA} > T_C^{RPA}$.

III. RESULTS AND DISCUSSION

A. Details of calculations

Potential functions and Green functions that appear in Eq. (3) were determined within the nonrelativistic TB-LMTO method in the so-called orthogonal representation[28] assuming the experimental lattice constants and the exchange potential in the form suggested by Vosko-Wilk-Nusair.[30] It should be noted that some calculations, in particular for T_C^{MFA}, were also done using the scalar-relativistic formulation. The contour integral along the path C that starts below the lowest occupied band and ends at the Fermi energy (we assume zero temperature) was calculated following the scheme described in Ref. 28 that employs the Gaussian quadrature method. Twenty energy nodes were used on the semicircle in the upper part of the complex energy plane. The integration over the full Brillouin zone was performed very carefully to obtain well-converged results even for very distant coordination shells (up to 172nd shell for fcc lattice and the 195th shell for bcc lattice). In particular, we have used up to 5×10^6 **k** points in the full Brillouin zone for the energy point on the contour C closest to the Fermi energy, and the number of **k** points then progressively decreased for more distant points, and for points close to the bottom of the band.

B. Effective Heisenberg exchange parameters

We will first discuss qualitatively the dependence of J_{ij} on the distance $R_{ij} = |\mathbf{R}_i - \mathbf{R}_j|$. In the limit of large values of R_{ij} the expression (3) can be evaluated analytically by means of the stationary-phase approximation.[31] For simplicity we consider here a single-band model but the results can be generalized also to the multiband case (see Ref. 32). For a large R_{ij} behaves g_{ij}^{σ} as

$$g_{ij}^{\sigma}(E + i0^+) \propto \frac{\exp[i(\mathbf{k}^{\sigma} \cdot \mathbf{R}_{ij} + \Phi^{\sigma})]}{R_{ij}}, \tag{12}$$

TABLE I. Effective Heisenberg exchange parameters J_{0j} for ferromagnetic Fe, Co, and Ni for the first 10 shells. Quantities $\mathbf{R}_{0j}$ and N_s denote, respectively, shell coordinates in units of corresponding lattice constants and the number of equivalent sites in the shell.

Fe (bcc)			Co (fcc)			Ni (fcc)		
$\mathbf{R}_{0j}$	N_s	J_{0j} (mRy)	$\mathbf{R}_{0j}$	N_s	J_{0j} (mRy)	$\mathbf{R}_{0j}$	N_s	J_{0j} (mRy)
$(\frac{1}{2}\frac{1}{2}\frac{1}{2})$	8	1.432	$(\frac{1}{2}\frac{1}{2}0)$	12	1.085	$(\frac{1}{2}\frac{1}{2}0)$	12	0.206
(100)	6	0.815	(100)	6	0.110	(100)	6	0.006
(110)	12	−0.016	$(1\frac{1}{2}\frac{1}{2})$	24	0.116	$(1\frac{1}{2}\frac{1}{2})$	24	0.026
$(\frac{3}{2}\frac{1}{2}\frac{1}{2})$	24	−0.126	(110)	12	−0.090	(110)	12	0.012
(111)	8	−0.146	$(\frac{3}{2}\frac{1}{2}0)$	24	0.026	$(\frac{3}{2}\frac{1}{2}0)$	24	0.003
(200)	6	0.062	(111)	8	0.043	(111)	8	−0.003
$(\frac{3}{2}\frac{3}{2}\frac{1}{2})$	24	0.001	$(\frac{3}{2}1\frac{1}{2})$	48	−0.024	$(\frac{3}{2}1\frac{1}{2})$	48	0.007
(210)	24	0.015	(200)	6	0.012	(200)	6	−0.001
(211)	24	−0.032	$(\frac{3}{2}\frac{3}{2}0)$	12	0.026	$(\frac{3}{2}\frac{3}{2}0)$	12	−0.011
$(\frac{3}{2}\frac{3}{2}\frac{3}{2})$	8	0.187	$(2\frac{1}{2}\frac{1}{2})$	24	0.006	$(2\frac{1}{2}\frac{1}{2})$	24	0.001

where $\mathbf{k}^\sigma$ is the wave vector of energy E in a direction such that the associated group velocity $\nabla_{\mathbf{k}}E^\sigma(\mathbf{k})$ is parallel to $\mathbf{R}_{ij}$, and Φ^σ denotes a corresponding phase factor. The energy integration in Eq. (3) yields additional factor of $1/R_{ij}$ (Ref. 31) and one obtains

$$J_{ij} \propto \mathrm{Im} \frac{\exp[\,i(\mathbf{k}_{\mathrm{F}}^{\uparrow}+\mathbf{k}_{\mathrm{F}}^{\downarrow})\cdot\mathbf{R}_{ij}+\Phi^{\uparrow}+\Phi^{\downarrow}]}{R_{ij}^3}. \tag{13}$$

For a weak ferromagnet both Fermi wave vectors $\mathbf{k}_{\mathrm{F}}^{\uparrow}$ and $\mathbf{k}_{\mathrm{F}}^{\downarrow}$ are real and one obtains a characteristic RKKY-like behavior

$$J_{ij} \propto \frac{\sin[\,(\mathbf{k}_{\mathrm{F}}^{\uparrow}+\mathbf{k}_{\mathrm{F}}^{\downarrow})\cdot\mathbf{R}_{ij}+\Phi^{\uparrow}+\Phi^{\downarrow}]}{R_{ij}^3}, \tag{14}$$

i.e., the exchange interaction has an oscillatory character with an envelope decaying as $1/R_{ij}^3$. On the other hand, for a strong ferromagnet with a fully occupied majority band the corresponding Fermi wave vector is imaginary, namely $\mathbf{k}_{\mathrm{F}}^{\uparrow} = i\boldsymbol{\kappa}_{\mathrm{F}}^{\uparrow}$ and one obtains an exponentially damped RKKY behavior

$$J_{ij} \propto \frac{\sin(\mathbf{k}_{\mathrm{F}}^{\downarrow}\cdot\mathbf{R}_{ij}+\Phi^{\uparrow}+\Phi^{\downarrow})\exp(-\boldsymbol{\kappa}_{\mathrm{F}}^{\uparrow}\cdot\mathbf{R}_{ij})}{R_{ij}^3}. \tag{15}$$

The qualitative features of these RKKY-type oscillations of J_{ij} will not be changed in realistic ferromagnets. For a weak ferromagnet, like Fe, one expects a pronounced RKKY character giving rise to strong Kohn anomalies in the spin-wave spectrum. On the other hand, for Co and Ni that are almost strong ferromagnets one expects a less pronounced RKKY character, less visible Kohn anomalies in the spin-wave spectrum (see Sec. III C), and faster decay of J_{ij} with a distance R_{ij}. It should be noted that due to the sp-d hybridization no itinerant ferromagnet is a truly strong ferromagnet.

The calculated Heisenberg exchange parameters J_{ij} for bcc Fe, fcc Co, and fcc Ni are presented in the Table I for the first ten shells. The exchange parameters J_{ij} for bcc Fe remain non-negligible over a very long range along the [111] direction, and change from ferromagnetic to antiferromagnetic couplings already for the third nearest neighbors (NN). In case of Co this change appears only for the 4th NN whereas Ni remains ferromagnetic up to the 5th NN. It should be noted a short range of J_{ij} for the case of Ni, being essentially a decreasing function of the distance with the exception of the second NN. Such behavior is in a qualitative agreement with conclusions obtained from the asymptotic behavior of J_{ij} with distance discussed above, in particular with the fact that bcc Fe is a weak ferromagnet while fcc Co and, in particular, fcc Ni are almost strong ferromagnets.

TABLE II. Calculated spin-wave stiffness constants (D_{th}) and Curie temperatures (T_C^{MFA} and T_C^{RPA}) and their comparison with experimental values D_{ex} and T_C^{ex}.

Metal	D_{th} (meV Å^2)	D_{ex} (meV Å^2)	T_C^{MFA} (K)	T_C^{RPA} (K)	T_C^{ex} (K)
Fe (bcc)	250±7	280,[a] 330[b]	1414	950±2	1044–1045
Co (fcc)	663±6	580,[c,a] 510[b]	1645	1311±4	1388–1398[c]
Ni (fcc)	756±29	555,[d] 422[a]	397	350±2	624–631

[a]Magnetization measurement (Ref. 37) at 4.2 K.
[b]Neutron-scattering measurement extrapolated to 0 K (Ref. 38).
[c]Data refer to hcp Co at 4.2 K.
[d]Neutron-scattering measurement at 4.2 K (Ref. 36).

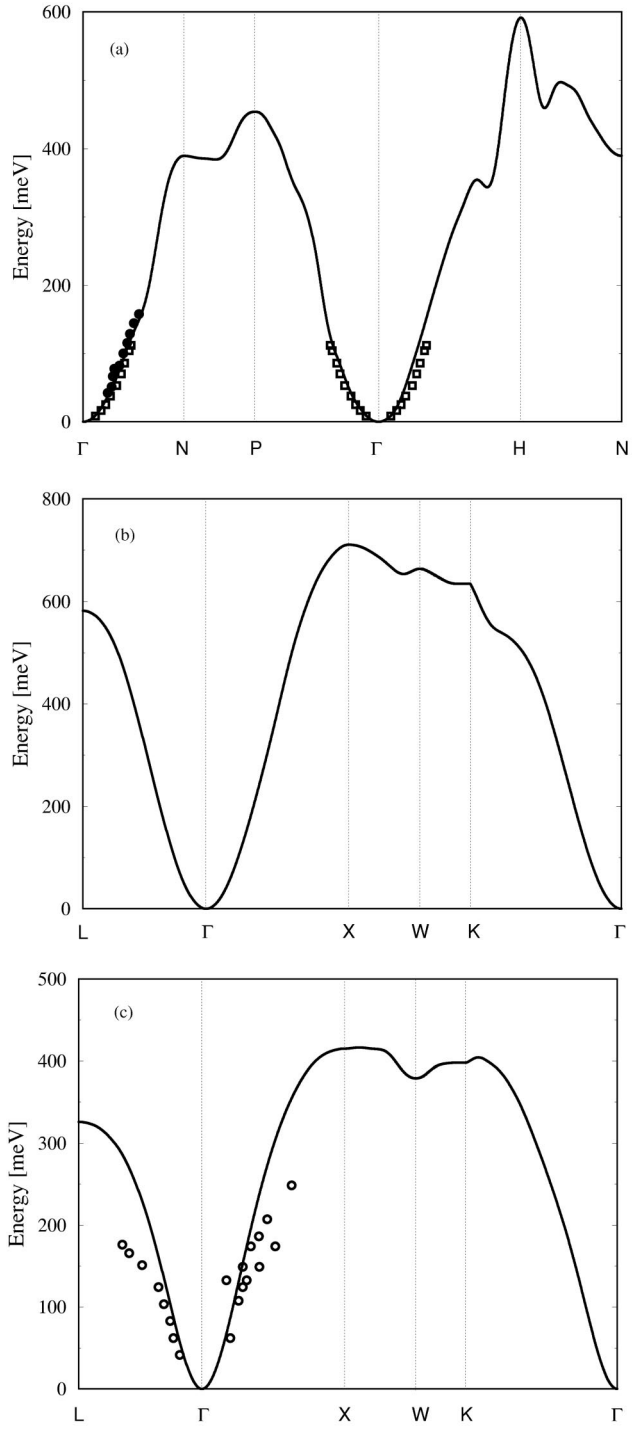

FIG. 1. Magnon-dispersion relations along high-symmetry lines in the Brillouin zone: (a) bcc Fe (experiment: Ref. 33, 10 K, filled circles and Ref. 35, Fe(12% Si), room temperature, empty squares); (b) fcc Co; and (c) fcc Ni (experiment: Ref. 34, room temperature, empty circles). Lines are calculated results.

There have been several previous calculations of J_{ij}'s for Fe and Ni.[2,5,7,11,26] Present calculations agree well with calculations of Refs. 2, 5, and 11, and there is also a reasonable agreement with results of Refs. 26 and 7. It should be mentioned that J_{ij} for both fcc Co and hcp Co were determined and they agree quite well with each other[7] (see also Table III below). Finally, we have also verified numerically the validity of an important sum rule, namely, $J_0=\Sigma_{i\neq 0}J_{0i}$. The sum fluctuates with the number of shells very weakly for, say, more than 50 shells.

C. Dispersion relations

Calculated magnons energy spectra $E(\mathbf{q})$ along the high-symmetry directions of the Brillouin zone are presented in Figs. 1(a–c) together with available experimental data.[33–35] We have used all calculated shells to determine $E(\mathbf{q})$, namely, 195 and 172 shells for bcc and fcc metals, respectively. Corresponding plot of $E(\mathbf{q})$ for fcc-Ni exhibits parabolic, almost isotropic behavior for long wavelengths and a similar behavior is also found for fcc Co. On the contrary, in bcc Fe we observe some anisotropy of $E(\mathbf{q})$, i.e., $E(\mathbf{q})$ increases faster along the Γ-N direction and more slowly along the Γ-P direction. In agreement with Refs. 4 and 7 we observe a local minima around the point H along Γ-H and H-N directions in the range of short wavelengths. They are indications of the so-called Kohn anomalies[4] that are due to long-range interactions mediated by the RKKY interactions similarly like Kohn-Migdal anomalies in phonon spectra are due to long-range interactions mediated by Friedel oscillations. It should be mentioned that minima in dispersion curve of bcc Fe appear only if the summation in Eq. (2) is done over a sufficiently large number of shells, in the present case for more than 45 shells. A similar observation concerning of the spin-wave spectra of bcc Fe was also done by Wang *et al.*[26] where authors used the fluctuating band theory method using semiempirical approach based on a fitting procedure for parameters of the Hamiltonian. On the other hand in a recent paper by Brown *et al.*[6] above-mentioned Kohn-anomalies in the behavior of spin-wave spectra of bcc Fe were not found, possibly because the spin-wave dispersion was obtained as an average over all directions in the $\mathbf{q}$ space.

Present results for dispersion relations compare well with available experimental data of measured spin-wave spectra for Fe and Ni.[33–35] For low-lying part of spectra there is also a good agreement of present results for dispersion relations with those of Refs. 4 and 7 obtained using the frozen-magnon approach. There are, however, differences for a higher part of spectra, in particular for the magnon bandwidth of bcc Fe that can be identified with the value of $E(\mathbf{q})$ evaluated at the high-symmetry point $\mathbf{q}=\mathbf{H}$ in the bcc-Brillouin zone. The origin of this disagreement is unclear. We have carefully checked the convergence of the magnon-dispersion laws $E(\mathbf{q})$ with the number of shells included in Eq. (2) and it was found to be weak for 50–70 shells and more. However, if the number of shells is small the differences may be pronounced, e.g., our scalar-relativistic calculations give for the bcc-Fe magnon bandwiths the values of 441 meV and 550 meV for 15 and 172 shells, respectively. The former value agrees incidentally very well with that given in Refs. 4 and 7. On the other hand, even small differences in values of $E(\mathbf{q})$ are strongly amplified when one evaluates the second derivative of $E(\mathbf{q})$ with respect to $\mathbf{q}$, i.e., the spin-wave stiffness constant. One should keep in

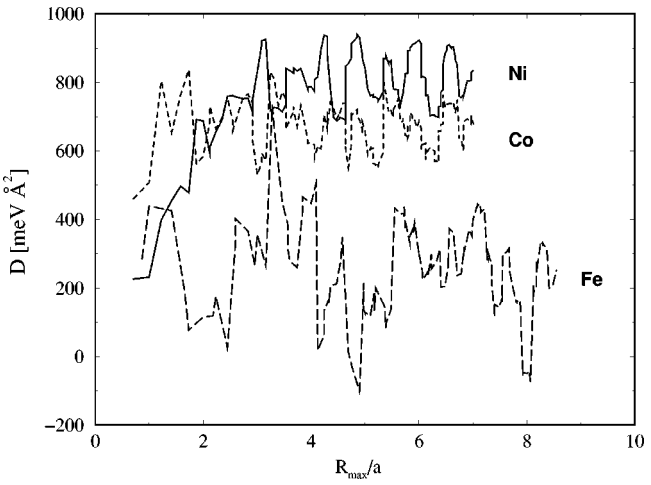

FIG. 2. Spin-wave stiffness constants calculated from Eq. (6) as a function of R_{max} (in units of lattice constants) for fcc Ni (full line), fcc Co (short dashes), and bcc Fe (long dashes).

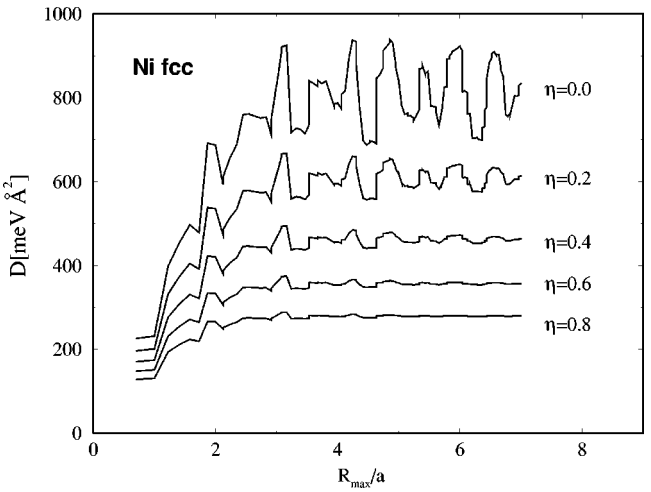

FIG. 3. Spin-wave stiffness of fcc Ni calculated from Eq. (16) as a function of R_{max} (in units of lattice constant) for various values of the damping factor η.

mind, however, that the above discussion is somehow academic, for it concerns an energy region where the adiabatic approximation ceases to be a good one, so that spin waves are no longer well defined because of their strong damping due to Stoner excitations (see, e.g., Ref. 5). The results of theoretical calculations based upon the adiabatic approximation can be thus compared with each other, but not with experimental data. It should be pointed out that the influence of deviations in the calculation of magnon spectra for large values of **q** of the Curie temperature is minimized for its RPA value as compared to its MFA value (see Eqs. (8) and (10)).

D. Spin-wave stiffness constant

As was already mentioned, the sum in Eq. (6) does not converge due to the characteristic RKKY behavior (14) and, therefore, Eq. (6) cannot be used directly to obtain reliable values for the spin-wave stiffness constant. This is demonstrated in Fig. 2 where the dependence of calculated spin-wave stiffness constants on the parameter R_{max} in Eq. (6) is plotted. The oscillatory character of D vs R_{max} persists for large values of R_{max} for the case of bcc Fe and even negative values of spin-wave stiffness constants were obtained for some values of R_{max}. To resolve this difficulty we suggest to regularize the expression (6) by substituting it by the formally equivalent expression that is, however, numerically convergent

$$D = \lim_{\eta \to 0} D(\eta),$$

$$D(\eta) = \lim_{R_{max} \to \infty} \frac{2\mu_B}{3M} \sum_{0 < R_{0j} \leqslant R_{max}} J_{0j} R_{0j}^2 \exp(-\eta R_{0j}/a). \tag{16}$$

The quantity η plays a role of a damping parameter that makes the sum over R_{ij} absolutely convergent as it is seen from Fig. 3. The quantity $D(\eta)$ is thus an analytical function of the variable η for any value $\eta > 0$ and can be extrapolated to the value $\eta = 0$. To show that the limit for $\eta \to 0$ is indeed finite and that our scheme is mathematically sound, let us consider as an example a typical RKKY interaction $J(R) \propto \sin(kR+\Phi)/R^3$. For large R we can employ Eq. (14) and substitute the sum in Eq. (6) by a corresponding integral. We obtain

$$\lim_{\eta \to 0} D(\eta) \propto 4\pi \int_{R_0}^{\infty} R^4 \frac{\sin(kR+\Phi)}{R^3} dR$$
$$= 4\pi R_0^2 [\cos(\Phi)\,\mathrm{si}''(kR_0) + \sin(\Phi)\,\mathrm{ci}''(kR_0)], \tag{17}$$

where $\mathrm{si}''(x)$ and $\mathrm{ci}''(x)$ denote the second derivative of integral sine and cosine, respectively. Since $\mathrm{si}(x)$ and $\mathrm{ci}(x)$ are analytical for $x \neq 0$, the integral is indeed finite.

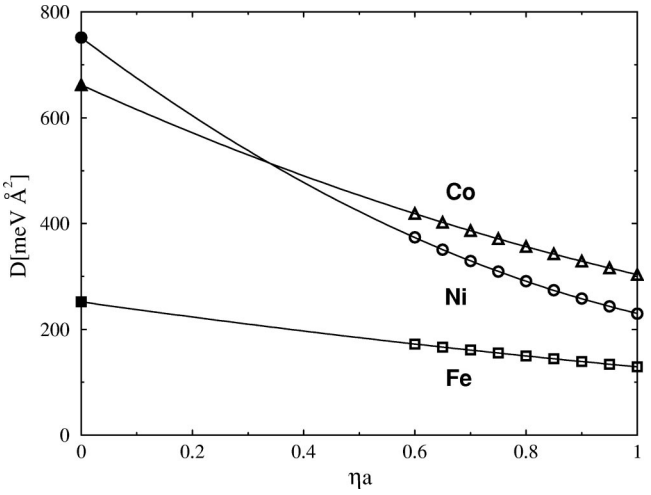

FIG. 4. Spin-wave stiffness coefficients $D(\eta)$ for bcc Fe (empty squares), fcc Co (empty triangles), and fcc Ni (empty circles) as a function of the parameter η and extrapolated values for $\eta = 0$ (filled symbols). The solid line indicates the quadratic fit function used for extrapolation.

TABLE III. Calculated Curie temperatures of ferromagnetic metals in the mean-field approximation for nonrelativistic (nr) and scalar-relativistic (sr) cases.

Metal	T_C^{nr} (K)	T_C^{sr} (K)
Fe (bcc)	1414	1335
Co (fcc)	1645	1651
Co (hcp)	1679	1673
Ni (fcc)	397	428

We therefore perform calculations for a set of values $\eta \in (\eta_{min}, \eta_{max})$ for which $D(\eta)$ is a smooth function with a well pronounced limit for large R_{max}. The limit $\eta=0$ is then determined at the end of calculations by a quadratic least-square extrapolation method. Typically, 5–15 values of η was used for $\eta_{min}\approx 0.5$–0.6 and $\eta_{max}\approx 0.9$–1.2 with a relative error of order of a few percent. In calculations we have used $R_{max}=7a$ for fcc and $9a$ for bcc, where a denotes the corresponding lattice constant. It should be noted a proper order of limits in Eq. (16), namely, first evaluate a sum for large R_{max} and then limit η to zero. The procedure is illustrated in Fig. 4. The results for spin-stiffness coefficient D calculated in this way are summarized in Table II together with available experimental data.[36–38] There is a reasonable agreement between theory and experiment for bcc Fe and fcc Co but the values of spin-wave stiffness constant are considerably overestimated for fcc Ni. It should be noted that measurements refer to the hcp Co while the present calculations were performed for fcc Co. A similar accuracy between calculated and measured spin-wave stiffness constants was obtained by Halilov *et al.*[4] using the frozen-magnon approach. Our results are also in a good agreement with those obtained by van Schilfgaarde and Antropov[7] using the spin-spiral calculations to overcome the problem of evaluation of D from Eq. (6). On the other hand, this problem was overlooked in Refs. 2, 13, and 14 so that a good agreement of D, calculated for a small number of coordination shells, with experimental data seems to be fortituous. Finally, results of Brown *et al.*[6] obtained by the layer Korringa-Kohn-Rostoker method in the frozen-potential approximation are underestimated for all metals and the best agreement is obtained for Ni.

E. Curie temperature

Several attempts have been made to evaluate Curie temperatures of magnetic transition metals[4,7,12,39,40] most of them based on the MFA. MFA as a rule overestimates values of Curie temperatures (with exception of fcc Ni with values substantially underestimated). We will show that an alternative method based on the Green function approach in the framework of the RPA (Refs. 22–25) can give a better agreement with experimental data. The RPA Curie temperatures were calculated from Eq. (11) by employing the method of analytical deconvolution.[29] In order to test the accuracy of this procedure we compare the present numerical results for the ratio T_C^{MFA}/T_C^{RPA} obtained for the nearest-neighbor Heisenberg model with the exact results:[22,25] we obtain 1.33 (fcc) and 1.37 (bcc) as compared to exact values 1.34 and 1.39, respectively, i.e., a numerical procedure agrees with exact results within 1% accuracy. Calculated values of Curie temperatures for both the MFA and RPA as well as corresponding experimental data are summarized in Table II. Mean-field values of Curie temperatures are overestimated for Fe and Co, but underestimated for Ni in agreement with other calculations.[4,7] On the other hand, the results obtained using the RPA approach are in a good agreement with experiment for both fcc Co and bcc Fe, while the results for fcc-Ni are even more underestimated. This is in agreement with the fact mentioned in Sec. II, namely, that $T_C^{RPA} < T_C^{MFA}$. The present results for Fe and Ni are in a good agreement with results of Ref. 20 using the spin-fluctuation theory and an improved statistical treatment in the framework of the Onsager cavity-field method.

The calculated ratio T_C^{MFA}/T_C^{RPA} is 1.49, 1.25, 1.13 for bcc Fe, fcc Co, and fcc Ni, respectively. The values differ from those obtained for the first-nearest-neighbor Heisenberg model due to non-negligible next-nearest neighbors in realistic ferromagnets and their oscillatory behavior with the shell number.

The last point concerns the relevance of relativistic corrections for the evaluation of the exchange parameters and related quantities. The simplest quantity to evaluate is the MFA value of the Curie temperature [see Eq. (9)]. Results for ferromagnetic metals (including hcp Co) are summarized in Table III by comparing the nonrelativistic and scalar-relativistic values. One can conclude that scalar-relativistic corrections are not important for fcc Co and hcp Co but their effect is non-negligible for fcc Ni and bcc Fe. The scalar-relativistic corrections generally shifts sp-bands downwards as compared to the d-band complex while the changes of magnetic moments are generally very small (a similar exchange splitting). One can thus ascribe above changes mostly to the modifications of the density of states at the Fermi energy [the site-diagonal blocks of the Green function in Eq. (9)]. Results also show only a weak dependence of the calculated T_C^{MFA} on the structure (hcp Co vs fcc Co).

F. Comparison between the real-space and frozen-magnon approaches

The real-space and frozen-magnon approaches are formally equivalent to each other. The quantities that are directly calculated (the J_{ij}'s in the former case, the $E(\mathbf{q})$'s in the latter) are related to each other by a Fourier transformation. Therefore, the pros and cons of both approaches concern mainly their computational efficiency.

The computational effort needed to obtain one J_{ij} parameter within the real-space approach is approximately the same as to compute one magnon energy $E(\mathbf{q})$ within the frozen-magnon approach: in both cases a fine Brillouin zone integration is required.

Therefore, it is quite clear that if one is primarily interested in spin-wave dispersion curves (for a moderate number of $\mathbf{q}$ points), or in the spin-wave stiffness D, the frozen-magnon approach is superior, for it does not require to perform a Fourier transformation and the delicate analysis ex-

plained in Sec. III D. We have shown, however, although less direct and computationally more demanding, the real-space approach performs well also.

On the other, if one is interested in the Curie temperature, the real-space approach is more efficient. This is obvious if one uses the mean-field approximation. Indeed, T_C^{MFA} is obtained from a *single* real-space calculation, by using the sum rule (9), whereas many $E(\mathbf{q})$'s are needed to obtain T_C^{MFA} from Eq. (8) within the frozen-magnon approach. Also if one uses the RPA, the real-space approach is more efficient. For both approaches, the integral over $\mathbf{q}$ in Eq. (10) needs to be performed accurately, with paying great attention to the divergence of the integrant at $\mathbf{q}=0$. A very high density of $\mathbf{q}$ points is required there, in order to have a satisfactory convergence. Within the frozen-magnon approach, each of the $E(\mathbf{q})$'s requires the same computational effort. In contrast, within the real-space approach, less than 200 J_{ij}'s are sufficient to obtain a parametrization of $E(\mathbf{q})$ over the full Brillouin zone, which considerably reduces the computational effort. Finally, the dependence of exchange parameters J_{ij} on the distance also gives an important information about the nature of the magnetic state (RKKY-like interactions) and this dependence is again straigtforwardly determined by the real-space method while in the reciproacal-space method J_{ij}'s have to be determined by inverting Eq. (2).

The real-space approach can be straightforwardly applied also to systems with a broken translational symmetry like, e.g., surfaces, overlayers, multilayers, and, in particular, to random substitutional alloys. This is an important advantage keeping in mind the relevance and yet not fully understood character of exchange interactions at metal interfaces and surfaces. It should be said, however, that the reciprocal-space approaches can also be applied to surfaces and interfaces via supercell approach, and, in particular, a fast algorithm for the evaluation of magnon spectra of complex solids that scales linearly with number of basis atoms has appeared recently with promissing future applications.[41]

Summarizing, the real-space and reciprocal-space approaches are, and in fact should be used as, complementary each to other and one has to choose the corresponding approach depending on the physical system and the quantity of interest in question, and the computational effort required. Conveniently, their results should be compared each to other if possible.

IV. SUMMARY

We have calculated Heisenberg exchange parameters of bcc Fe, fcc Co, and fcc Ni in real space from first principles by employing the magnetic force theorem. We have determined dispersion curves of magnetic excitations along high-symmetry directions in the Brillouin zone, spin-wave stiffness constants, and Curie temperatures of considered metals on the same footing, namely, all based on calculated values of exchange parameters J_{ij}. Dispersion curves of bcc Fe exhibit an anisotropic behavior in the range of long wavelengths, with peculiar minima for short wavelengths in the [100] direction that are due to a relatively strong exchange oscillations in this metal. We have presented a method of evaluation of the spin-wave stiffness constants that yields converged values, in contrast to previous results in the literature. Calculated spin-wave stiffness constants agree reasonably well with available experimental data for Co and Fe, while agreement is rather poor for Ni. Present calculations agree also well with available experimental data for magnon-dispersion law of bcc Fe. We have also evaluated Curie temperatures of metals in question using the mean-field approximation and the Green-function random-phase approximation. We have found that in the latter case a good agreement with the experiment is obtained for Co and Fe, while less satisfactory results are obtained for Ni, where the role of the Stoner excitations is much more important as compared to Co and Fe. In addition, the adiabatic approximation is less justified for Ni, and, possibly, correlation effects beyond the local-density approximation play the more important role for this ferromagnet.

In conclusion, we have demonstrated that the real-space approach is able to determine the low-lying excitations in ferromagnetic metals with an accuracy comparable to the reciprocal-space approach. This justifies the use of the real-space approach for more interesting and complex systems with violated translational symmetry like, e.g., the thin magnetic films on nonmagnetic substrates and, in particular, the random magnetic alloys in general. The first promising application of the real-space approach to the problem of the oscillatory Curie temperature of two-dimensional ferromagnets has been recently published.[42]

ACKNOWLEDGMENTS

J.K., V.D., and I.T. acknowledge financial support provided by the Grant Agency of the Academy of Sciences of the Czech Republic (Project A1010829), the Grant Agency of the Czech Republic (Project 202/00/0122), and the Czech Ministry of Education, Youth, and Sports (Projects OC P3.40 and OC P3.70).

[1] A.I. Liechtenstein, M.I. Katsnelson, and V.A. Gubanov, J. Phys. F: Met. Phys. **14**, L125 (1984).

[2] A.I. Liechtenstein, M.I. Katsnelson, V.P. Antropov, and V.A. Gubanov, J. Magn. Magn. Mater. **67**, 65 (1987).

[3] V.P. Antropov, M.I. Katsnelson, B.N. Harmon, M. van Schilfgaarde, and D. Kusnezov, Phys. Rev. B **54**, 1019 (1996).

[4] S.V. Halilov, H. Eschrig, A.Y. Perlov, and P.M. Oppeneer, Phys. Rev. B **58**, 293 (1998).

[5] V.P. Antropov, B.N. Harmon, and A.N. Smirnov, J. Magn. Magn. Mater. **200**, 148 (1999).

[6] R.H. Brown, D.M.C. Nicholson, X. Wang, and T.C. Schulthess, J. Appl. Phys. **85**, 4830 (1999).

[7] M. van Schilfgaarde and V.P. Antropov, J. Appl. Phys. **85**, 4827 (1999).
[8] O. Ivanov and V.P. Antropov, J. Appl. Phys. **85**, 4821 (1999).
[9] J.M. MacLaren, T.C. Schulthess, W.H. Butler, R. Sutton, and M. McHenry, J. Appl. Phys. **85**, 4833 (1999).
[10] B. Újfalussy, X.-D. Wang, D.M.C. Nicholson, W.A. Shelton, G.M. Stocks, Y. Wang, and B.L. Gyorffy, J. Appl. Phys. **85**, 4824 (1999).
[11] S. Frota-Pessoa, R.B. Muniz, and J. Kudrnovský, Phys. Rev. B **62**, 5293 (2000).
[12] A. Sakuma, J. Phys. Soc. Jpn. **68**, 620 (1999).
[13] D. Spišiak and J. Hafner, J. Magn. Magn. Mater. **168**, 257 (1997).
[14] V.P. Antropov, M.J. Katsnelson, B.N. Harmon, and A.I. Liechtenstein, Physica B **237**, 336 (1997).
[15] P.H. Dederichs, S. Blügel, R. Zeller, and H. Akai, Phys. Rev. Lett. **53**, 2512 (1984).
[16] Q. Niu and L. Kleinman, Phys. Rev. Lett. **80**, 2205 (1998).
[17] Q. Niu, X. Wang, L. Kleinman, W.-M. Liu, D.M.C. Nicholson, and G.M. Stocks, Phys. Rev. Lett. **83**, 207 (1999).
[18] A. Oswald, R. Zeller, P.J. Braspenning, and P.H. Dederichs, J. Phys. F: Met. Phys. **15**, 193 (1985).
[19] L.M. Sandratskii, J. Phys.: Condens. Matter **3**, 8565 (1991).
[20] J.B. Staunton and B.L. Gyorffy, Phys. Rev. Lett. **69**, 371 (1992).
[21] S. V Tyablikov, *Methods of Quantum Theory of Magnetism* (Plenum Press, New York, 1967).
[22] R.A. Tahir-Kheli and D. ter Haar, Phys. Rev. **127**, 88 (1962).
[23] R.A. Tahir-Kheli, Phys. Rev. **132**, 689 (1963).
[24] H.B. Callen, Phys. Rev. **130**, 890 (1963).
[25] R.A. Tahir-Kheli and H.S. Jarrett, Phys. Rev. **135**, A1096 (1964).
[26] C.S. Wang, R.E. Prange, and V. Korenman, Phys. Rev. B **25**, 5766 (1982).
[27] O.K. Andersen and O. Jepsen, Phys. Rev. Lett. **53**, 2571 (1984).
[28] I. Turek, V. Drchal, J. Kudrnovský, M. Šob, and P. Weinberger, *Electronic Structure of Disordered Alloys, Surfaces and Interfaces*, (Kluwer, Boston, 1997); I. Turek, J. Kudrnovský, and V. Drchal, in *Electronic Structure and Physical Properties of Solids*, Vol. 535 of Lecture Notes in Physics, edited by H. Dreyssé (Springer, Berlin, 2000), p. 349.
[29] K.S. Haas, B. Velický, and H. Ehrenreich, Phys. Rev. B **29**, 3697 (1984).
[30] S.H. Vosko, L. Wilk, and M. Nusair, Can. J. Phys. **58**, 1200 (1980).
[31] P. Bruno, Phys. Rev. B **52**, 411 (1995).
[32] J. Kudrnovský, V. Drchal, I. Turek, P. Bruno, P. H. Dederichs, and P. Weinberger, in *Electronic Structure and Physical Properties of Solids*, (Ref. 28), p. 313.
[33] C.K. Loong, J.M. Carpenter, J.W. Lynn, R.A. Robinson, and H.A. Mook, J. Appl. Phys. **55**, 1895 (1984).
[34] H.A. Mook and D.McK. Paul, Phys. Rev. Lett. **54**, 227 (1985).
[35] J.W. Lynn, Phys. Rev. B **11**, 2624 (1974).
[36] H.A. Mook, J.W. Lynn, and M.R. Nicklow, Phys. Rev. Lett. **30**, 556 (1973).
[37] R. Pauthenet, J. Appl. Phys. **53**, 2029 (1982); **53**, 8187 (1982).
[38] G. Shirane, V.J. Minkiewicz, and R. Nathans, J. Appl. Phys. **39**, 383 (1968).
[39] J. Hubbard, Phys. Rev. B **19**, 2626 (1979); **20**, 4584 (1980); **23**, 5974 (1981).
[40] M.V. You, V. Heine, A.J. Holden, and P.J. Lin-Chung, Phys. Rev. Lett. **44**, 1282 (1980).
[41] O. Grotheer, C. Ederer, and M. Fähnle, Phys. Rev. B **63**, 100401(R) (2001).
[42] M. Pajda, J. Kudrnovský, I. Turek, V. Drchal, and P. Bruno, Phys. Rev. Lett. **85**, 5424 (2000).